CANCER BIOTHERAPY AND RADIOPHARMACEUTICALS
Volume 28, Number 7, 2013

DOI: 10.1089/cbr.2013.1487

Original Articles

ImmunoPET Imaging of Renal Cell Carcinoma with ^{124}I- and ^{89}Zr-Labeled Anti-CAIX Monoclonal Antibody cG250 in Mice

Alexander B. Stillebroer,[1,2] Gerben M. Franssen,[1] Peter F.A. Mulders,[2] Wim J.G. Oyen,[1] Guus A.M.S. van Dongen,[3] Peter Laverman,[1] Egbert Oosterwijk,[2] and Otto C. Boerman[1]

Abstract

Introduction: Monoclonal antibody (mAb) cG250 recognizes carbonic anhydrase IX (CAIX), overexpressed on clear cell renal cell carcinoma (ccRCC). ^{124}I-cG250 is currently under clinical investigation for the detection of ccRCC. However, the ^{124}I label is rapidly excreted from the tumor cells after internalization of the radiolabeled mAb. We hypothesized that labeling cG250 with the residualizing positron emitter ^{89}Zr would lead to higher tumor uptake and more sensitive detection of ccRCC lesions.
Materials and Methods: Nude mice with CAIX-expressing ccRCC xenografts (SK-RC-52 or NU-12) were i.v. injected with ^{89}Zr-cG250 or ^{124}I-cG250. To determine specificity of ^{89}Zr-cG250 uptake in ccRCC, one control group was i.v. injected with ^{89}Zr-MOPC21 (irrelevant mAb). PET images were acquired using a small animal PET camera and the biodistribution of the radiolabeled mAb was determined.
Results: The ccRCC xenografts were clearly visualized after injection of ^{89}Zr-cG250 and ^{124}I-cG250. Tumor uptake of ^{89}Zr-cG250 was significantly higher compared with ^{124}I-cG250 in the NU-12 tumor model (114.7% ± 25.2% injected dose per gram (%ID/g) vs. 38.2 ± 18.3%ID/g, $p = 0.029$), but in the SK-RC-52 the difference in tumor uptake was not significant (48.7 ± 15.2%ID/g vs. 32.0 ± 22.9%ID/g, $p = 0.26$). SK-RC-52 tumors were not visualized with ^{89}Zr-MOPC21 (tumor uptake 3.0%ID/g). Intraperitoneal SK-RC-52 lesions as small as 7 mm^3 were visualized with ^{89}Zr-cG250 PET.
Conclusion: ImmunoPET imaging with cG250 visualized s.c. and i.p. ccRCC lesions in murine models. This confirms the potential of cG250 immunoPET in the diagnosis and (re)staging of ccRCC. PET imaging of ccRCC tumors with ^{89}Zr-cG250 could be more sensitive than ^{124}I-cG250-PET.

Key words: ^{124}I, ^{89}Zr, cG250, immunoPET

Introduction

Renal cell carcinoma (RCC) accounts for 2% of all malignancies and the current treatment for localized disease is tumor nephrectomy. When metastasized, prognosis is bleak with a median survival of 12 months.[1] With the advent of targeted agents (e.g., sunitinib, sorafenib and temsirolimus), it is crucial to adequately diagnose and (re)stage RCC. Considering that a number of patients have long-lasting stable disease without treatment, adequate timing of when to start these treatments is crucial, because considerable toxicities are associated with the use of these targeted agents.[2] The preoperative characterization of renal lesions suspect for RCC is difficult with the current radiological techniques. Moreover, since conventional radiological follow-up may not be adequate for response assessment of targeted agents,[3] new techniques are warranted to assess biological tumor changes and hence, predict the response to treatment.

The diagnosis and (re)staging of RCC is currently performed with conventional radiological techniques, such as

Departments of [1]Nuclear Medicine and [2]Urology, Radboud University Nijmegen Medical Centre, Nijmegen, The Netherlands.
[3]Department of Otolaryngology/Head and Neck Surgery, VU University Medical Center, Amsterdam, The Netherlands.

Address correspondence to: Otto C. Boerman; Department of Nuclear Medicine, Radboud University Nijmegen Medical Centre; Gert Gooteplein 8, 6525 GA Nijmegen, The Netherlands
E-mail: **o.boerman@nucmed.umcn.nl**

computed tomography (CT) or ultrasound. The diagnosis of primary RCC by FDG PET is hampered by the low FDG-avidity of RCC and the physiologic uptake in the normal kidneys due to the renal clearance of the tracer.[4] FDG PET has been studied in a small number of patients for the detection and follow-up of RCC metastases. Although a high specificity was reported, sensitivity was relatively low and FDG PET is now considered unsuited for staging of patients with RCC.[4]

Monoclonal antibody (mAb) cG250 has a high affinity for carbonic anhydrase IX (CAIX), a tumor-associated antigen ubiquitously expressed on clear cell RCC (ccRCC).[5] The use of cG250 in radioimmunoscintigraphy and radioimmunotherapy to detect or treat ccRCC has been investigated extensively.[6–10] A few investigations have studied the capabilities of cG250-based immunoPET, that is, combining the favorable characteristics of PET (high spatial resolution, three-dimensional (3D) imaging and accurate quantification of tumor uptake) with the high and specific targeting of cG250 to CAIX-expressing cells.[11–13] The relatively slow pharmacokinetics of i.v. injected radiolabeled mAbs (optimal tumor uptake after several days) prevents the use of the most commonly used positron emitters (^{11}C and ^{18}F) because their half-lives (20 and 110 minutes, respectively) are too short to be used in immunoPET. The half-lives of the positron emitters ^{89}Zr (T½ = 78 hours, mean $\beta+$ 397 keV (23% yield), γ 909 keV), and ^{124}I (T½ = 100 hours, mean $\beta+$ 824 keV (23% yield), γ 603 (63% yield) and 722/1691 keV (10% yield) do match the relatively slow kinetics of antibodies. In a prospective study by Divgi *et al.*, twenty-five patients with suspect renal lesions scheduled for nephrectomy were studied with ^{124}I-cG250. Of 16 patients with pathologically confirmed ccRCC after surgery, 15 had a positive scan (tumor-to-normal kidney ratio ≥3:1). The failure in one patient was attributed to technical problems with the labeled material. The study showed that ^{124}I-cG250 could aid in the preoperative characterization of suspect renal masses and might guide crucial aspects of surgical RCC management.[11] A large multicenter trial comparing conventional diagnostic CT to ^{124}I-cG250 immunoPET/CT for the detection of ccRCC in 226 patients scheduled for nephrectomy showed a significantly higher rate of ccRCC detection with ^{124}I-cG250 immunoPET/CT over conventional CT ($p = 0.016$).[14]

We hypothesized that, due to its residualizing characteristics and favourable lower beta+emission, labeling cG250 with ^{89}Zr instead of ^{124}I will lead to higher tumor uptake, higher tumor-to-background (T/B) ratios and higher PET resolution and hence, more accurate detection of ccRCC lesions.

Here we studied the biodistribution of ^{89}Zr-Df-cG250 and ^{124}I-cG250 in nude mice with subcutaneous (s.c.) ccRCC xenografts. FDG PET was used as a reference in this study. The specific targeting of cG250 to ccRCC was assessed by comparing tumor uptake of ^{89}Zr-Df-cG250 and an irrelevant control mAb. The feasibility of ^{89}Zr-immunoPET with ^{89}Zr-Df-cG250 was studied in mice with intraperitoneally growing ccRCC tumors.

Materials and Methods

Chimeric mAb G250

The isolation and immunohistochemical reactivity of mAb G250 have been described elsewhere.[15] To reduce the immunogenicity of the murine form of G250, a chimeric version (cG250) has been developed.[10] MAb cG250 IgG1 is reactive with the transmembrane glycoprotein carbonic anhydrase isoenzyme IX ($K_a = 4 \times 10^9\ M^{-1}$). Expression on the cell surface of ccRCC cells is ubiquitous (>95%), whereas expression on normal tissues is restricted to the epithelial structures of the upper gastrointestinal tract and larger bile ducts.[16]

Murine mAb MOPC21

MOPC21 is a myeloma-produced murine IgG1 mAb (Sigma-Aldrich, Zwijndrecht, The Netherlands), which is not directed against any known antigen and was used as an isotype control mAb to investigate the specificity of uptake of mAb cG250 in CAIX-positive ccRCC xenografts.

Conjugation, radiolabeling, and quality control

For ^{89}Zr labeling, cG250 and MOPC21 were conjugated with desferal (Df) essentially as described previously.[17] Briefly, desferal (Novartis Pharma AG, Bern, Switzerland) was succinylated, temporarily filled with Fe^{3+} and coupled to the mAb via the tetrafluorophenolester of Df. After the conjugation of Df to the mAb and removal of the Fe^{3+}, the Df-conjugated mAb was labeled with ^{89}Zr (IBA Pharma, Leuven, Belgium) during 30 minutes in 0.25 M HEPES buffer, at pH 7.3 at 37°C. The ^{89}Zr-Df-cG250 and ^{89}Zr-Df-MOPC21 were purified on a PD10 column (Amersham Pharmacia Biotech, Uppsala, Sweden), that was eluted with 0.9% NaCl, 5 mg/mL gentisic acid, pH 5.0. The specific activity of ^{89}Zr-Df-cG250 was 0.41 MBq/μg or 0.54 MBq/μg.

Radioiodination of cG250 with ^{124}I (IBA Pharma, Leuven, Belgium) was performed according to the Iodogen method.[10] The ^{124}I-cG250 was purified on a PD-10 column that was eluted with 0.5 M PBS. Specific activity of ^{124}I-cG250 was 0.24 MBq/μg or 1.7 MBq/μg.

Labeling efficiency was between 55 and 70% (^{89}Zr-Df-cG250/MOPC21) and between 73 and 82% (^{124}I-cG250). After purification, at the time of i.v. injection, instant thin layer chromatography showed a radiochemical purity of >95% of all preparations used in the studies. The immunoreactive fraction at infinite antigen excess of all radiolabeled cG250 preparations was determined on freshly trypsinized SK-RC-52 RCC cells essentially as described by Lindmo *et al.*[18] The immunoreactive fraction of ^{89}Zr-Df-cG250 was between 75% and 89% and the immunoreactive fractions of all ^{124}I-cG250 preparations exceeded 83%.

RCC tumors in nude mice

The ccRCC cell lines SK-RC-52 (CAIX-positive) and SK-RC-59 (CAIX-negative) were derived from metastases of primary ccRCC patients as described by Ebert *et al.*[19] To induce s.c. tumors, 2–3.10^6 cells were injected subcutaneously in the flank of 6–8 weeks old male BALB/c nu/nu mice and tumors were established after 2–3 weeks. To obtain intraperitoneally growing SK-RC-52 lesions, 2–3.10^6 SK-RC-52 cells were injected intraperitoneally and after 3 weeks multiple tumor nodules were found in the abdominal cavity. The ccRCC cell line NU-12 (CAIX-positive) was derived from a primary ccRCC[20] and tumors were noted 6–8 weeks after serial s.c. transplantation. Animals were housed and fed according to the Dutch animal welfare regulations. Experiments were

approved by the Institutional Animal Care and Use Committee of the Radboud University Nijmegen Medical Centre, and were performed in accordance with their guidelines.

MicroPET imaging

Mice with s.c. SK-RC-52 tumors were i.v. injected with 12.3 MBq ^{89}Zr-Df-cG250/MOPC21 (30 μg) or 7.2 MBq ^{124}I-cG250 (30 μg).[21] Mice with s.c. NU-12 tumors were i.v. injected with 1.5 MBq ^{89}Zr-Df-cG250 (3 μg) or 5.1 MBq ^{124}I-cG250 (3 μg).[21] Mice injected with FDG (IBA, Amsterdam, The Netherlands) received 10 MBq. PET images were acquired with a dedicated animal PET/CT scanner (Inveon, Siemens Preclinical Solutions, Knoxville, TN) with an intrinsic spatial resolution of 1.5 mm. Mice were placed in a prone (experiments 1 and 2) or supine (experiment 3) position in the scanner and body temperature was maintained at 37°C using a warmed mattress (M2M imaging, Inc., Cleveland, OH). Scans were reconstructed using Inveon Acquisition Workplace software version 1.2 (Siemens Preclinical Solutions, Knoxville, TN). PET reconstruction was performed using an ordered subset expectation maximization-3D/maximum a posteriori (OSEM3D/MAP) algorithm.[22] All animals were gas-anesthetized with a mixture of nitrous oxide/oxygen/isoflurane. Before intravenous injection of FDG, mice were fasted 6 hours. Emission images after injection of FDG were acquired 1 hour p.i. CT images were acquired with the same Inveon animal PET/CT scanner (80 kV, 500 μA, exposure time 300 milliseconds, 360° rotation in 180 steps, 0.5 mm aluminum filter). Scans were reconstructed using COBRA software version 6 (Exxim Computing Corporation, Pleasanton, CA). CT acquisition was performed 7 days after injection of ^{89}Zr-Df-cG250, ^{89}Zr-Df-MOPC21 and ^{124}I-cG250, or 1 hour after injection of [^{18}F]FDG.

At the end of the experiments (1 hour p.i. of FDG or 7 days p.i. of ^{89}Zr-Df-cG250, ^{89}Zr-Df-MOPC21, and ^{124}I-cG250) mice were euthanized and the biodistribution of the radiolabel was determined. Tumor and samples of normal tissues (blood, muscle, lung, spleen, kidney, liver, small intestine, stomach, and thyroid) were dissected, weighed, and counted in a γ-counter (1480 Wizard 3'', LKB/Wallace, Perkin-Elmer, Boston, MA). Injection standards were counted simultaneously to correct for radioactive decay.

Biodistribution studies

Biodistribution of ^{89}Zr-Df-cG250 and ^{124}I-cG250 was studied in mice with either a s.c. SK-RC-52 or NU-12 tumor using FDG as reference. Six groups of mice were studied, with three groups bearing a s.c. SK-RC-52 tumor and three groups bearing a s.c. NU-12 tumor. Groups consisted of six mice and were injected with ^{89}Zr-Df-cG250, ^{124}I-cG250, or FDG (1.5–12.3 MBq/mouse).

The specificity of cG250-targeting to CAIX-expressing ccRCC tumors was evaluated in two groups of mice with a s.c. SK-RC-52 tumor (CAIX-positive) in the left flank and a s.c. SK-RC-59 tumor (CAIX-negative) in the right flank. One group of mice received ^{89}Zr-Df-cG250 (12.3 MBq/mouse), the other group received ^{89}Zr-Df-MOPC21 (12.3 MBq/mouse).

To determine immunoPET imaging of intraperitoneally growing ccRCC lesions six mice with i.p. SK-RC-52 tumors were injected with ^{89}Zr-Df-cG250 (16.2 MBq/mouse).

Statistical analysis

Statistical analysis was performed using the nonparametric repeated measures one-way analysis of variance (ANOVA). Differences were considered significant when $p < 0.05$, two-sided. All values are expressed as mean ± standard deviation (SD).

Results

The biodistribution of ^{89}Zr-Df-cG250 and ^{124}I-cG250 7 days after injection in mice with CAIX-expressing ccRCC tumors is summarized in Figure 1. In the NU-12 tumor model, tumor uptake of ^{89}Zr-Df-cG250 was significantly higher compared with ^{124}I-cG250 (114.7 ± 25.2%ID/g vs. 38.2 ± 18.3%ID/g, respectively, $p = 0.029$) (Fig. 1A), whereas in the SK-RC-52 tumor model uptake of ^{89}Zr-Df-cG250 and ^{124}I-cG250 was similar (48.7 ± 15.2%ID/g vs. 32.0 ± 22.9%ID/g, respectively, $p = 0.257$) (Fig. 1B). When comparing the biodistribution of ^{89}Zr-Df-cG250 with that of ^{124}I-cG250, uptake of ^{89}Zr-Df-cG250 was higher in liver ($p < 0.001$) and spleen ($p < 0.001$) and uptake of ^{124}I was higher in the thyroid ($p < 0.001$) in both models. Uptake of the two cG250 preparations in other organs did not differ significantly. PET images of mice injected with ^{89}Zr-Df-cG250 and ^{124}I-cG250 are shown in Figure 2. Tumors were

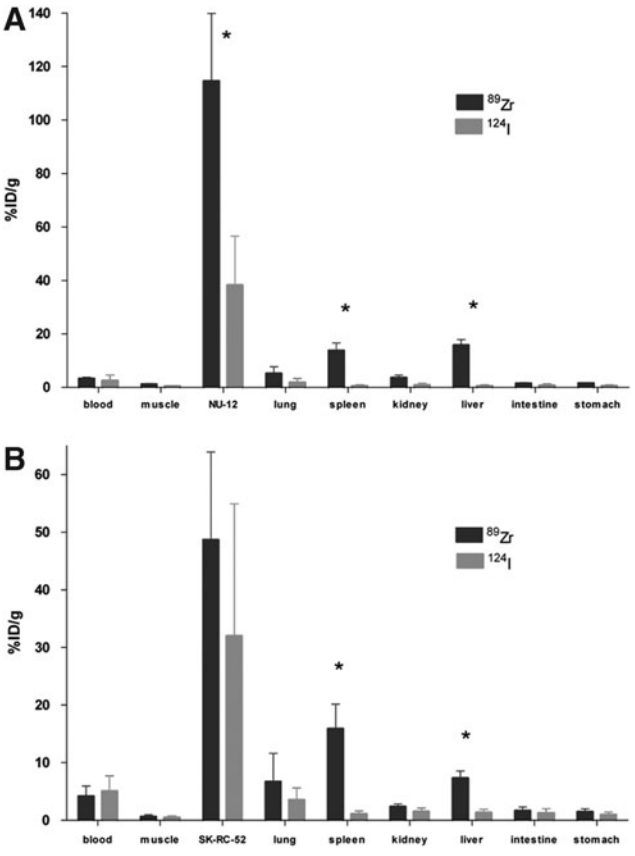

FIG. 1. Biodistribution of ^{89}Zr-Df-cG250 and ^{124}I-cG250 in mice with a s.c. NU-12 tumor **(A)** or a s.c. SK-RC-52 tumor **(B)**, 7 days p.i. Values are expressed as mean ± SD. Antibody protein dose was 3 μg cG250/mouse in NU-12 and 30 μg cG250/mouse in SK-RC-52 tumors. Significant differences ($p < 0.05$) in uptake between ^{89}Zr-Df-cG250 and ^{124}I-cG250 are marked with an asterisk*.

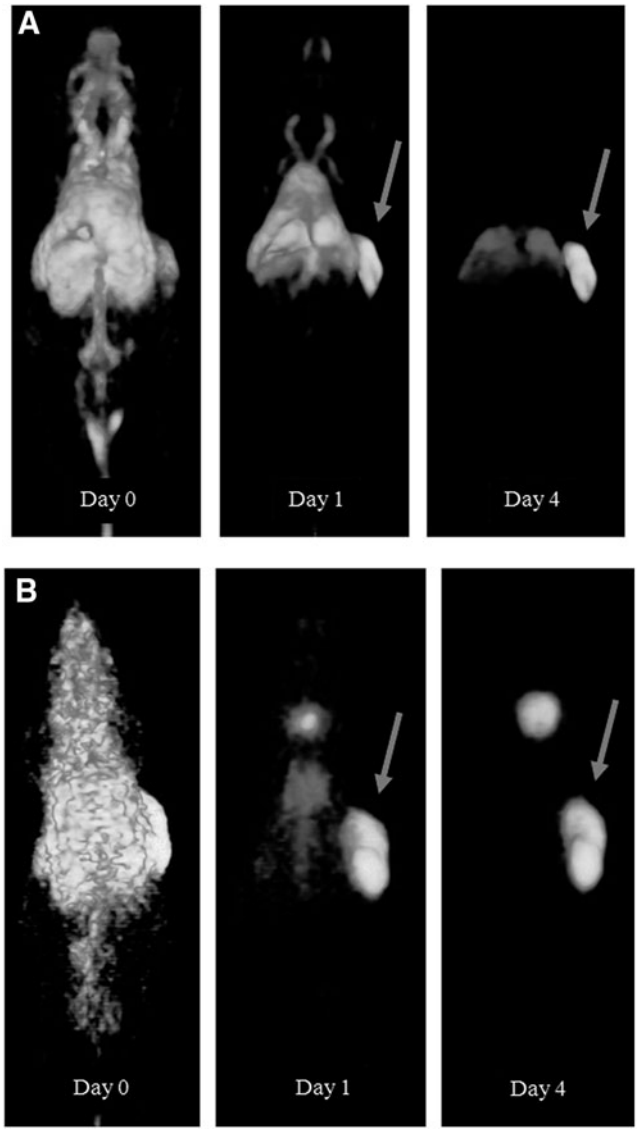

FIG. 2. Three dimensional (3D) reconstructed PET images of representative mice with a s.c. NU-12 tumor on the right flank 0, 1, and 4 days after injection and fused PET/CT images after 7 days of 3 μg ^{89}Zr-Df-cG250 **(A)** or 3 μg ^{124}I-cG250 **(B)**. Note the clear visualization of the s.c. tumor (arrows) from day 1 p.i. onwards with both radiolabeled mAbs.

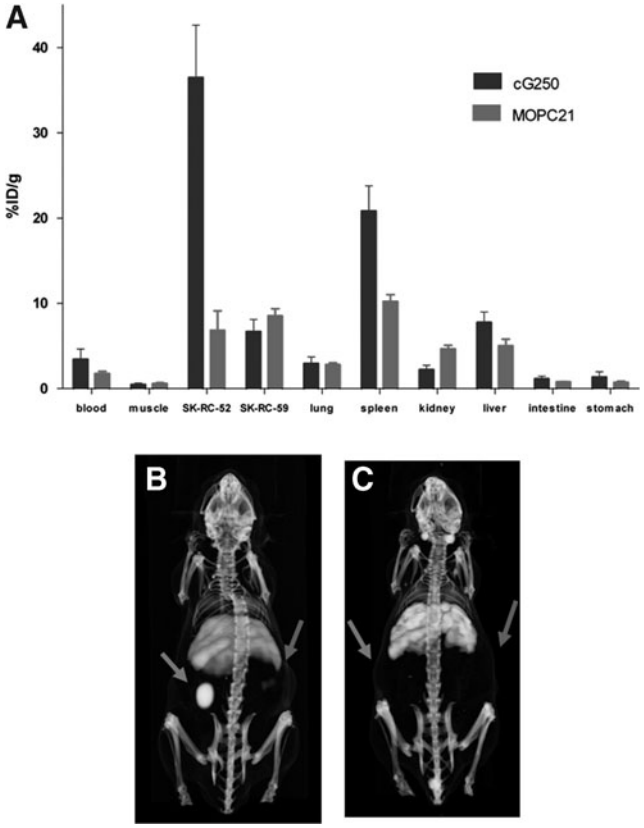

FIG. 3. Biodistribution, 7 days after injection of 30 μg ^{89}Zr-Df-cG250 or ^{89}Zr-Df-MOPC21 in mice with a s.c. SK-RC-52 tumor and a s.c. SK-RC-59 tumor **(A)**. Values are expressed as mean ± SD 3D. Reconstructed PET/CT images 7 days p.i. ^{89}Zr-Df-cG250 **(B)** or ^{89}Zr-Df-MOPC21 **(C)** in representative mice with a s.c. SK-RC-52 tumor on the left flank and a s.c. SK-RC-59 tumor on the right flank. Note the high uptake of ^{89}Zr-Df-cG250 in the SK-RC-52 tumor (left arrow), which is not seen in the SK-RC-59 tumor (right arrow). No specific uptake in both tumors is noted after injection with ^{89}Zr-Df-MOPC21.

visualized from day 1 onwards with both radiolabeled antibody preparations and optimal image contrast was seen day 7 p.i. The physical characteristics of ^{124}I caused noisier and lower contrast images. Uptake of FDG in the NU-12 and SK-RC-52 tumors was relatively low (2.7 ± 0.5%ID/g vs. 5.7 ± 3.9%ID/g) and both tumors were not visualized on PET images since uptake in the tumor was similar to that in surrounding tissues (results not shown).

The biodistribution of ^{89}Zr-Df-cG250 and ^{89}Zr-Df-MOPC21 7 days p.i. were compared to determine the specificity of cG250 localization in CAIX-positive tumors (Fig. 3A). Uptake of ^{89}Zr-Df-cG250 in the CAIX-positive SK-RC-52 tumor was high (36.5 ± 6.2%ID/g), whereas the uptake was significantly lower in the CAIX-negative SK-RC-59 tumor (6.7 ± 1.4%ID/g, $p = 0.029$). Uptake of ^{89}Zr-Df-cG250 and ^{89}Zr-Df-MOPC21 differed significantly in the CAIX-positive SK-RC-52 tumor (36.5 ± 6.2%ID/g vs. 6.8 ± 2.3%ID/g, $p = 0.010$), indicating that the uptake of ^{89}Zr-Df-cG250 in the CAIX-positive tumor was due to the affinity of the cG250 antibody for CAIX. PET images of mice with s.c. SK-RC-52 and SK-RC-59 tumors injected with ^{89}Zr-Df-MOPC21 or ^{89}Zr-Df-cG250 are shown in Figure 3B. The CAIX-positive SK-RC-52 tumor was clearly visualized with ^{89}Zr-Df-cG250 on day 7 p.i. The CAIX-negative SK-RC-59 tumor was not visualized with ^{89}Zr-Df-cG250. None of the s.c. tumors was visualized with the irrelevant mAb ^{89}Zr-Df-MOPC21. These results demonstrate the specific localization of ^{89}Zr-Df-cG250 in CAIX-positive tumors.

Intraperitoneally growing SK-RC-52 tumors were clearly visualized 7 days after injection of ^{89}Zr-Df-cG250 as shown in Figure 4. Tumor lesions as small as 7 mg in the vicinity of the liver and spleen were clearly visualized and uptake in individual lesions was as high as up to 95.9%ID/g. All tumor lesions that were identified with PET were identified during dissection.

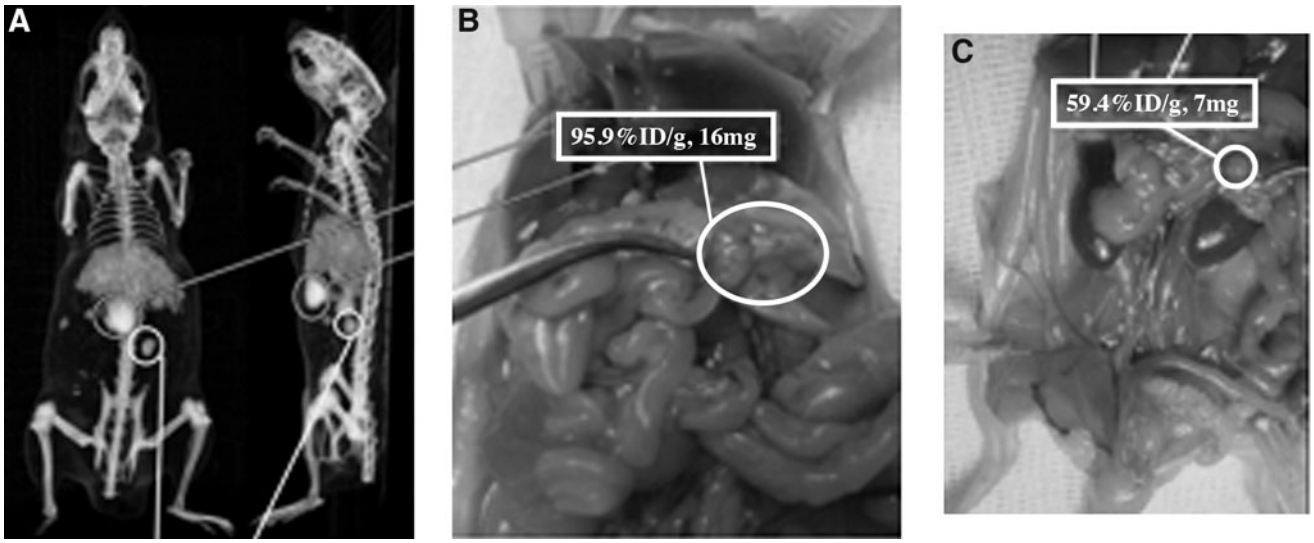

FIG. 4. **(A)** Coronal and sagittal sections of a 3D reconstructed PET/CT image 7 days after injection of ^{89}Zr-Df-cG250 and **(B)** anatomical localization of an SK-RC-52 lesion (circle) upon dissection with an uptake of 95.9%ID/g, weight 16 mg. **(C)** Localization of another SK-RC-52 lesion (circle) with 59.4%ID/g uptake, weight 7 mg.

Discussion

The biodistribution profiles of ^{89}Zr-Df-cG250 and ^{124}I-cG250 in nude mice with s.c. ccRCC xenografts were compared to determine the optimal radionuclide for immunoPET with cG250. In both CAIX-positive ccRCC xenografts, uptake of ^{89}Zr-Df-cG250 was higher than uptake of ^{124}I-cG250 7 days after injection of the radiolabeled mAbs, albeit this difference was only statistically significant in the NU-12 tumor model. In this study, mice were not stratified to groups according to size of the tumor xenograft. The group bearing a SK-RC-52 xenograft injected with ^{124}I-cG250 consisted of mice with large differences in tumor size (results not shown), evidenced by the large standard deviation in tumor uptake of this group. This could explain why uptake of ^{89}Zr-Df-cG250 was not significantly higher than ^{124}I-cG250 in the SK-RC-52 tumor model. PET images acquired with a dedicated small animal PET camera showed preferential tumor uptake of both radiolabeled mAbs from day 1 p.i. onwards and image contrast improved with time. The images obtained with ^{89}Zr-Df-cG250 had less noise and higher contrast, allowing for more specific detection of ccRCC lesions with ^{89}Zr-Df-cG250 as compared to ^{124}I-cG250. The brightness and contrast settings of the ^{89}Zr-Df-cG250-images in Figure 2 have been chosen specifically to show the uptake in the liver for anatomical reference. Moreover, since uptake of ^{89}Zr-Df-cG250 in ccRCC lesions was higher compared with ^{124}I-cG250, immunoPET imaging of ccRCC with ^{89}Zr-Df-cG250 in these models was superior to immunoPET with ^{124}I-cG250.

The enhanced uptake of ^{89}Zr-Df-cG250 as compared to ^{124}I-cG250 in the NU-12 ccRCC tumor model is most likely due to the residualizing properties of the ^{89}Zr radiolabel. Internalized radiolabeled antibody is metabolized in the tumor cell lysosomes and the ^{124}I-labeled metabolite (^{124}I-tyrosine) is rapidly excreted from the tumor cell, whereas the metabolite labeled with metallic radionuclides, such as ^{111}In, ^{89}Zr and ^{177}Lu, is trapped in the lysosomes.[23–25] This phenomenon has also been described in a clinical intrapatient comparison study examining the differences between ^{131}I-cG250 and ^{111}In-cG250. Five mRCC patients were injected with ^{131}I-cG250 and ^{111}In-cG250 1 week apart. Uptake of ^{111}In-cG250 in ccRCC tumor lesions was higher compared with ^{131}I-cG250, which was attributed to the intracellular entrapment of internalized ^{111}In-cG250 metabolites.[7] This could also explain the higher liver and spleen uptake of ^{89}Zr-Df-cG250 as compared to that of ^{124}I-cG250.[26,27]

FDG PET has a poor sensitivity for detecting RCC lesions mainly due to the fact that many RCC lesions are not FDG-avid.[4] This was also observed in the present study: none of the CAIX-positive ccRCC xenografts were visualized by FDG PET, since uptake of FDG was similar to that in surrounding tissues. In an earlier study, FDG failed to visualize ccRCC xenografts in nude rats.[12] ImmunoPET with cG250 could therefore, be of value as a functional imaging technique to detect ccRCC lesions.

The high tumor uptake of ^{89}Zr-Df-cG250 and ^{124}I-cG250 was the result of specific uptake of cG250 in the CAIX-positive tumors. The irrelevant mAb ^{89}Zr-Df-MOPC21 did not accumulate in the CAIX-positive tumor SK-RC-52, demonstrating that accretion was not the consequence of aberrant tumor perfusion, but antigen-driven. ^{89}Zr-Df-cG250 accumulated in the CAIX-positive tumor, but not in the CAIX-negative tumor, further demonstrating that accretion was antigen-driven.

ImmunoPET with cG250 is well suited for imaging ccRCC in patients since PET has the advantage of producing 3D images with a much higher resolution than planar scintigraphy or single photon emission computed tomography (SPECT). This is illustrated by the very sensitive detection of ccRCC lesions with a dedicated small animal PET camera. Intraperitoneal lesions as small as 7 mm^3 were visualized with ^{89}Zr-Df-cG250 and could easily be discriminated from the liver and spleen. Preoperative characterization of renal masses with cG250 immunoPET might be useful in the clinical management of RCC patients.[11] The results from this study suggest that immunoPET in RCC patients may be improved by using ^{89}Zr-Df-cG250 instead of ^{124}I-cG250.

Conclusions

Our results indicate that uptake of ^{89}Zr-Df-cG250 in ccRCC xenografts was higher than uptake of ^{124}I-cG250. The higher specific uptake of ^{89}Zr-Df-cG250 produced higher PET image contrast, despite higher uptake in various normal tissues, such as the liver and spleen. PET imaging of ccRCC tumors with ^{89}Zr-cG250 could be more sensitive than ^{124}I-cG250-PET. Small intraperitoneal ccRCC lesions could be visualized and easily discriminated from the liver and the spleen with cG250-based immunoPET.

Acknowledgments

MAb cG250 was a kind donation from Dr. P. Bevan (Wilex AG, München, Germany). The authors wish to thank B. Lemmers-van de Weem and K. Lemmens-Hermans for their assistance in the animal experiments. This work was supported by a grant from the Dutch Cancer Foundation (KWF grant KUN 2005–3339).

Disclosure Statement

One competing interest should be reported; E. Oosterwijk, works as a part-time consultant for Wilex AG, manufacturer of mAb cG250.

References

1. Jemal A, Siegel R, Ward E, et al. Cancer statistics, 2009. CA Cancer J Clin 2009;59:225.
2. Hartmann JT, Haap M, Kopp HG, et al. Tyrosine kinase inhibitors - a review on pharmacology, metabolism and side effects. Curr Drug Metab 2009;10:470.
3. Griffin N, Gore ME, Sohaib SA. Imaging in metastatic renal cell carcinoma. AJR Am J Roentgenol 2007;189:360.
4. Powles T, Murray I, Brock C, et al. Molecular positron emission tomography and PET/CT imaging in urological malignancies. Eur Urol 2007;51:1511.
5. Grabmaier K, Vissers JL, De Weijert MC, et al. Molecular cloning and immunogenicity of renal cell carcinoma-associated antigen G250. Int J Cancer 2000;85:865.
6. Brouwers AH, van Eerd JE, Frielink C, et al. Optimization of radioimmunotherapy of renal cell carcinoma: Labeling of monoclonal antibody cG250 with ^{131}I, ^{90}Y, ^{177}Lu, or ^{186}Re. J Nucl Med 2004;45:327.
7. Brouwers AH, Buijs WC, Oosterwijk E, et al. Targeting of metastatic renal cell carcinoma with the chimeric monoclonal antibody G250 labeled with (131)I or (111)In: An intrapatient comparison. Clin Cancer Res 2003;9:3953s.
8. Brouwers AH, Mulders PF, De Mulder PH, et al. Lack of efficacy of two consecutive treatments of radioimmunotherapy with 131I-cG250 in patients with metastasized clear cell renal cell carcinoma. J Clin Oncol 2005;23:6540.
9. Steffens MG, Boerman OC, De Mulder PH, et al. Phase I radioimmunotherapy of metastatic renal cell carcinoma with 131I-labeled chimeric monoclonal antibody G250. Clin Cancer Res 1999;5:3268s.
10. Steffens MG, Boerman OC, Oosterwijk-Wakka JC, et al. Targeting of renal cell carcinoma with iodine-131-labeled chimeric monoclonal antibody G250. J Clin Oncol 1997;15:1529.
11. Divgi CR, Pandit-Taskar N, Jungbluth AA, et al. Preoperative characterisation of clear-cell renal carcinoma using iodine-124-labelled antibody chimeric G250 (124I-cG250) and PET in patients with renal masses: A phase I trial. Lancet Oncol 2007;8:304.
12. Brouwers A, Verel I, Van EJ, et al. PET radioimmunoscintigraphy of renal cell cancer using 89Zr-labeled cG250 monoclonal antibody in nude rats. Cancer Biother Radiopharm 2004;19:155.
13. Lawrentschuk N, Lee FT, Jones G, et al. Investigation of hypoxia and carbonic anhydrase IX expression in a renal cell carcinoma xenograft model with oxygen tension measurements and (124)I-cG250 PET/CT. Urol Oncol 2011; 29:411.
14. Divgi CR, Uzzo RG, Gatsonis C, et al. Positron emission tomography/computed tomography identification of clear cell renal cell carcinoma: Results from the REDECT trial. J Clin Oncol 2013;31:187.
15. Oosterwijk E, Ruiter DJ, Hoedemaeker PJ, et al. Monoclonal antibody G 250 recognizes a determinant present in renal-cell carcinoma and absent from normal kidney. Int J Cancer 198615;38:489.
16. Thiry A, Dogne JM, Masereel B, et al. Targeting tumor-associated carbonic anhydrase IX in cancer therapy. Trends Pharmacol Sci 2006;27:566.
17. Verel I, Visser GW, Boellaard R, et al. 89Zr immuno-PET: Comprehensive procedures for the production of 89Zr-labeled monoclonal antibodies. J Nucl Med 2003;44:1271.
18. Lindmo T, Boven E, Cuttitta F, et al. Determination of the immunoreactive fraction of radiolabeled monoclonal antibodies by linear extrapolation to binding at infinite antigen excess. J Immunol Methods 1984;72:77.
19. Ebert T, Bander NH, Finstad CL, et al. Establishment and characterization of human renal cancer and normal kidney cell lines. Cancer Res 1990;50:5531.
20. Beniers AJ, Peelen WP, Schaafsma HE, et al. Establishment and characterization of five new human renal tumor xenografts. Am J Pathol 1992;140:483.
21. Kranenborg MH, Boerman OC, De Weijert MC, et al. The effect of antibody protein dose of anti-renal cell carcinoma monoclonal antibodies in nude mice with renal cell carcinoma xenografts. Cancer 1997;80:2390.
22. Visser EP, Disselhorst JA, Brom M, et al. Spatial resolution and sensitivity of the Inveon small-animal PET scanner. J Nucl Med 2009;50:139.
23. Sharkey RM, Behr TM, Mattes MJ, et al. Advantage of residualizing radiolabels for an internalizing antibody against the B-cell lymphoma antigen, CD22. Cancer Immunol Immunother 1997;44:179.
24. Shih LB, Thorpe SR, Griffiths GL, et al. The processing and fate of antibodies and their radiolabels bound to the surface of tumor cells *in vitro*: A comparison of nine radiolabels. J Nucl Med 1994;35:899.
25. Press OW, Shan D, Howell-Clark J, et al. Comparative metabolism and retention of iodine-125, yttrium-90, and indium-111 radioimmunoconjugates by cancer cells. Cancer Res 1996;56:2123.
26. Perk LR, Vosjan MJ, Visser GW, et al. p-Isothiocyanatobenzyl-desferrioxamine: A new bifunctional chelate for facile radiolabeling of monoclonal antibodies with zirconium-89 for immuno-PET imaging. Eur J Nucl Med Mol Imaging 2010; 37:250.
27. Verel I, Visser GW, Boellaard R, et al. Quantitative 89Zr immuno-PET for *in vivo* scouting of 90Y-labeled monoclonal antibodies in xenograft-bearing nude mice. J Nucl Med 2003; 44:1663.